

Liquid Surface Wave Band Structure Instabilities

Tom Chou

DAMTP, University of Cambridge, Cambridge CB3 9EW, United Kingdom

(Received 9 June 1997)

We study interfacial instabilities between two spatially periodically sheared ideal fluids. Bloch wave function decompositions of the surface deformation and fluid velocities result in a non-Hermitian secular matrix with an associated band structure that yields both linear oscillating and nonoscillating instabilities, enhanced near Bragg planes corresponding to the periodicity determined by converging or diverging surface flows. The instabilities persist *even* when the dynamical effects of the upper fluid are neglected, in contrast to the uniform shear Kelvin-Helmholtz (KH) instability. Periodic flows can also couple with uniform shear and *suppress* standard KH instabilities. [S0031-9007(97)04749-2]

PACS numbers: 47.20.Ft, 47.20.Ma, 68.10.-m

When two fluids of different density are uniformly sheared, a Kelvin-Helmholtz (KH) instability, where the interface deforms, may arise [1]. In this Letter, we exploit an analogy with solid state physics employing Bloch's theorem which allows us to calculate the coupling between *spatially periodic* shear and surface capillary-gravity waves. Regular fluid flow patterns are ubiquitous [2] in nature and can exist in parameter regimes prior to the onset of chaotic or turbulent flows. For example, Rayleigh-Bénard convection cells arise when heating of a fluid layer from below provides buoyancy [3] driving the instability. Regular convective rolls in the form of rectangles and hexagons can appear [3,4].

Periodic flows also occur in Langmuir circulation (LC) windrows where wind stresses, turbulent stresses, and Coriolis forces conspire to form convection rolls in the upper ocean [5]. These flows can be spatially periodic as often observed when the sea surface is contaminated by oil, algae, or air bubbles [6]. On larger scales are nearly periodic solar convection cells in stellar convective zones; here, magnetic fields may also affect the surface wave dynamics [7]. Thus, surface wave propagation and interfacial stability is an important aspect of stratified fluids with wide applicability and their dynamics may be a way of probing underlying flows.

Besides the large body of work on nonlinear surface waves and surface instabilities, linear oscillatory instabilities of the two-layer Bénard problem have been theoretically studied including thermal and Marangoni modes [4]. In the limiting one fluid Rayleigh-Bénard problem, with fixed lower temperature and fixed upper thermal flux, Benguria and Depassier [8] found interfacial oscillatory instabilities for parameters *prior* to the onset of the periodic roll states. Capillary-gravity wave instabilities in the presence of shear wind profiles [9], and flow over wavy bottoms [10] have also been considered. However, there has been no general treatment of surface wave propagation in the presence of fully developed periodic convection.

Here, we assume a preexisting periodic flow and explore its dynamical effects on interfacial instabilities. We

treat the surface waves as being reflected or refracted much like wave scattering in optical, acoustic, or electronic solid state physics, where band structures have been calculated using linear eigenvalue analyses [11]. A related problem of periodic surface wave scatterers such as thin ice floes has been treated with similar methods [12]. Here, the underlying *flow* is periodic so we use Bloch functions to describe the surface displacements and dynamic fluid pressure and derive a quadratic eigenvalue equation with an associated non-Hermitian operator. Within the nontrivial "band structure" we find a complex eigenvalue spectrum corresponding to linear instabilities that persist even in the one-fluid limit.

Formulation.—Consider two ideal fluids separated by a flat wave-undisturbed interface at $z = 0$ as shown in Fig. 1. Although the underlying flow field is typically rotational, we assume the flow associated with the imposed surface waves are irrotational. The surface wave displacements are assumed small and do not affect the underlying "quenched" flow. This requirement, and linearization, implies $\eta \ll \lambda, a$, where η , λ , and a are typical surface amplitudes, wavelengths, and flow field periodicities, respectively.

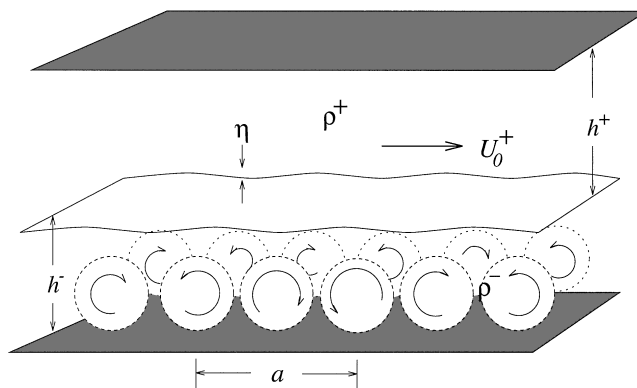


FIG. 1. Schematic of two ideal fluids separated by an interface with surface tension σ under the action of gravity. The densities, velocities, and depths of the upper and lower fluids are ρ^\pm , U^\pm , and h^\pm , respectively.

The fluid velocities above and below the interface are $\vec{v}^\pm = \vec{U}^\pm + \nabla\varphi^\pm$, where \vec{U}^\pm are the periodic flow fields (generated, for example, by the Rayleigh-Bénard instabilities [3], Langmuir circulation mechanisms [5], or electrohydrodynamic effects [13]) satisfying $\nabla \cdot \vec{U}^\pm = 0$, φ^\pm are the velocity potentials for the irrotational capillary-gravity waves, and $z = \pm h^\pm$ is the position of the impenetrable, flat top (bottom) boundaries. For concreteness, consider Rayleigh-Bénard instabilities to periodic flows in the free surface Boussinesq approximation which arise when $Ra \equiv \alpha g h^3 \Delta T / \nu \kappa > Ra^* \simeq 1100$, where α , g , ΔT , ν , and κ are the thermal expansion coefficient, gravitational acceleration, temperature difference $T(z=0) - T(z=-h)$, kinematic viscosity, and thermal conductivity, respectively. The ideal fluid approximation is valid only for surface waves which are not significantly damped over many periods of the underlying flow, e.g., for capillary waves, the attenuation length $k_d^{-1} \equiv 3\sigma / (4\nu\rho\omega) \gg a$.

Incompressibility demands $\nabla \cdot \vec{v}^\pm = \Delta\varphi^\pm = 0$, where $\Delta \equiv \Delta_\perp + \partial_z^2$ is the three-dimensional Laplacian. The linearized kinematic boundary conditions at $z = \pm h^\pm$ and the interface at $z \simeq 0$ are $\partial_z \varphi^\pm(\vec{x}, z = \mp h) = 0$ and

$$\partial_t \eta(\vec{r}) + \vec{U}^\pm(\vec{r}) \cdot \nabla_\perp \eta(\vec{r}) = \lim_{z \rightarrow 0^\pm} \partial_z \varphi^\pm(\vec{r}, z), \quad (1)$$

respectively [1], where $\vec{r}_\perp \equiv \vec{r} \equiv (x, y)$. The linearized dynamic boundary condition at $z \simeq 0$ is found by balancing z -component stresses from the dynamical pressure with those from gravity and surface tension:

$$\lim_{z \rightarrow 0^\pm} [\partial_t \varphi^\pm + U^\pm \partial_t \varphi^\pm] = \frac{\sigma}{\rho^\pm} \Delta_\perp \eta - g\eta, \quad (2)$$

where we have for simplicity neglected any possible Marangoni effects that may arise when surfactants are surface convected and assumed a constant surface tension σ . Spatially varying surface tension or bending rigidity can be treated straightforwardly [12,14]. Henceforth, we work in the frequency domain where all quantities vary as $e^{-i\omega t}$. Wave evolution due to a nontime harmonic

source can be found by superposing the solutions of many frequency components. The general solutions to $\varphi^\pm(\vec{r}, z)$ and $\eta(\vec{r})$ are

$$\varphi^\pm = \sum_{\vec{q}} \varphi_{\vec{q}}^\pm e^{i\vec{q} \cdot \vec{r}} \frac{\cosh q(h^\pm \mp z)}{\cosh qh^\pm}, \quad \eta = \sum_{\vec{q}} \eta_{\vec{q}} e^{i\vec{q} \cdot \vec{r}}, \quad (3)$$

where $\vec{q} \equiv \vec{q}_\perp$ lies in the surface plane, and $q \equiv \lim_{\epsilon \rightarrow 0} \sqrt{q^2 + \epsilon^2}$. Equation (3) automatically satisfies $\Delta\varphi^\pm = 0$ as well as the boundary conditions at $z = \pm h^\pm$. Therefore, the problem is reduced to that of simultaneously solving Eqs. (1) and (2) with the unknowns $\varphi_{\vec{q}}^\pm$ and $\eta_{\vec{q}}$. A Fourier decomposition for the periodic flows is

$$\vec{U}(\vec{r}, z) = \sum_{\vec{G}} \vec{U}(\vec{G}, z) e^{i\vec{G} \cdot \vec{r}}, \quad (4)$$

where \vec{G} are the reciprocal lattice vectors appropriate for the underlying flow periodicity. With (4), the velocity potential φ will also satisfy Bloch's theorem [11]: $\varphi(\vec{r}, z) = e^{i\vec{q} \cdot \vec{r}} f(\vec{r}, z)$, where $f(\vec{r})$ is a function invariant with respect to translations of \vec{a} .

Substituting Eqs. (3) and (4) into (1) and (2), and shifting the reciprocal wave vectors into the first Brillouin zone, we obtain

$$\sum_{\vec{G}'} (\mathbf{A}\omega^2 + \mathbf{B}\omega + \mathbf{C}) \eta_{\vec{q}}(\vec{G}') = 0, \quad (5)$$

where the matrices in the limit of unbounded upper fluid ($h^+ = \infty$, $h^- \equiv h$) are given by

$$A(\vec{G}, \vec{G}') \equiv (s \tanh|\vec{q} - \vec{G}|h + 1) \delta_{\vec{G}, \vec{G}'}, \quad (6)$$

$$B(\vec{G}, \vec{G}') \equiv -2s\vec{U}_0^+ \cdot (\vec{q} - \vec{G}) \tanh|\vec{q} - \vec{G}|h \delta_{\vec{G}, \vec{G}'} - \left(1 + \frac{|\vec{q} - \vec{G}| \tanh|\vec{q} - \vec{G}|h}{|\vec{q} - \vec{G}'| \tanh|\vec{q} - \vec{G}'|h} \right) \times \vec{U}^-(\vec{G} - \vec{G}') \cdot (\vec{q} - \vec{G}'), \quad (7)$$

$$C(\vec{G}, \vec{G}') \equiv [s|\vec{U}_0^+ \cdot (\vec{q} - \vec{G})|^2 \tanh|\vec{q} - \vec{G}|h - \Omega_{\vec{q}}^2(\vec{G})] \delta_{\vec{G}, \vec{G}'} + \sum_{\vec{G}''} \frac{|\vec{q} - \vec{G}| \tanh|\vec{q} - \vec{G}|h}{|\vec{q} - \vec{G}''| \tanh|\vec{q} - \vec{G}''|h} \times \vec{U}^-(\vec{G} - \vec{G}'') \cdot (\vec{q} - \vec{G}'') \vec{U}^-(\vec{G}'' - \vec{G}') \cdot (\vec{q} - \vec{G}'), \quad (8)$$

where $s \equiv \rho^+ / \rho^-$, and

$$\Omega_{\vec{q}}^2(\vec{G}) = \left(\frac{\sigma}{\rho^-} |\vec{q} - \vec{G}|^3 + (1-s)g|\vec{q} - \vec{G}| \right) \times \tanh|\vec{q} - \vec{G}|h. \quad (9)$$

Upon defining $\vec{\psi} \equiv \omega \vec{\eta}$, we arrive at an eigenvalue problem,

$$\begin{pmatrix} \mathbf{0} & \mathbf{1} \\ -\mathbf{A}^{-1}\mathbf{C} & -\mathbf{A}^{-1}\mathbf{B} \end{pmatrix} \begin{pmatrix} \vec{\eta}_{\vec{q}} \\ \vec{\psi}_{\vec{q}} \end{pmatrix} = \omega \begin{pmatrix} \vec{\eta}_{\vec{q}} \\ \vec{\psi}_{\vec{q}} \end{pmatrix}, \quad (10)$$

that can be solved by standard means [15]. Because (10) is non-Hermitian, the corresponding dispersion relation

$\omega(\vec{q})$ is complex. The standard criteria for the Kelvin-Helmholtz propagating wave instability is recovered when $\vec{U}^\pm = \vec{U}_0^\pm$ are uniform [1]:

$$(\omega - \vec{U}_0^- \cdot \vec{k})^2 + s \tanh kh (\omega - \vec{U}_0^+ \cdot \vec{k})^2 - \Omega_k^2(0) = 0. \quad (11)$$

Note that when dynamical effects of the upper fluid are neglected, ($s = 0$), the roots of Eq. (11) are real, and no linear instability exists.

Results and Discussion.—Distances, frequencies ω , and velocities U will be normalized and measured in units of a , $\sqrt{g/a}$, and \sqrt{ga} , respectively. First consider only periodic flow in the lower fluid with no uniform component, $\vec{U}^\pm(\vec{G} = 0) = 0$. Only the velocity at the surface $\vec{U}^-(\vec{r}, z = 0)$ will influence surface wave propagation. For simplicity we analyze one-dimensional rolls approximately described by

$$\vec{U}^-(\vec{r}, z = 0) = U^-(z)\hat{x} \cos\left(\frac{2\pi}{a}x\right); \quad (12)$$

consequently, $\vec{U}^-(\vec{G}) = U^-(0)\hat{x}/2\pi$ for $\vec{G} = \pm 2\pi\hat{x}/a$, and zero otherwise. This choice of phase for $\vec{U}^-(\vec{r}, z = 0)$ implies one converging and one diverging surface flow region per unit cell and also simplifies the computation by making all elements of the matrix in Eq. (10) real. Using standard methods [15], we find the spectrum of (10) and obtain the band structure for surface capillary-gravity waves with underlying periodic flows \vec{U}^- .

The central panels in Fig. 2 show the real (solid lines) and imaginary (height of hatched regions centered about $\text{Re}\{\omega\}$) parts of $\omega(q_x, 0)$; here, $\vec{U}_0^\pm = 0$, $h = 2.0$, $s = 0$, and the inverse Bond number $\text{Bo}^{-1} \equiv \sigma/\rho^- a^2 g = 0.01$ (which corresponds to $a \sim 2\text{--}3$ cm for water or light alcohols; also the requirement $k_d^{-1} \gg a$ is also satisfied). We use the notation $q(k)$ to denote quantities plotted in the reduced (extended) zone scheme. The side panels show $\omega(0, k_y)$ in the direction parallel to the rolls. The

choice of $U^-(\pm 2\pi/a) = 0.20, 0.75$ shown in 2(a) and 2(b) corresponds to surface velocities of ~ 9 and 30 cm/s. The band structures shown in Fig. 2(a) contain branch cuts at certain q_x satisfying the Bragg scattering condition. There are open band gaps at $q_x = 0$, which decrease at larger ω , similar to electronic and acoustic wave propagation in periodic media; the gaps normally found at $q_x = \pm\pi$ are collapsed due to the converging flow in each unit cell and are degenerate down to a smaller value of q_x . Under this periodic flow, growing surface modes arise near $q_x \sim \pm\pi$ when real degenerate roots of Eq. (10) split into complex conjugate pairs. Even though for the one fluid problem, *uniform stream* flows are stable according to (11), remarkably, an interface overlying periodic flows is generally linearly unstable, *even if* $\rho^+ = 0$. Periodic flows with finite \vec{G} couple with, and feed energy into, finite wave vector surface waves.

In Fig. 2(b), $|U^-(\pm 2\pi/a)| = 0.75$, and the first gap at $q_x = 0$ has also merged. Note that unstable modes are associated with both standing and low group velocity traveling waves since they appear predominantly near $q_x = 0, \pi$. These are damped or saturated by a contribution from viscous dissipation, $\text{Im}\{\omega\} \approx 2\nu|\vec{q} - \vec{G}|^2$. For $\vec{U}^-(2\pi/a) < 0.3641$, the band structure qualitatively resembles that of Fig. 2(a). When $0.417 > \vec{U}^-(2\pi/a) > 0.3641$, the lowest two branches collapse such that unstable zero frequency modes (i.e., $\text{Re}\{\omega(q_x, k_y)\} = 0$, $\text{Im}\{\omega(q_x, k_y)\} < 0$) proliferate and fill the whole zone. These growing modes are static surface deformations similar to the Reynolds ridge [16]. Upon further increasing $\vec{U}^-(2\pi/a) > 0.417$, the zero frequency growing modes develop a finite frequency and stabilize near $q_x \sim 0$. When $\vec{U}^-(2\pi/a) \approx 0.428$, the first gap at $q_x = 0$ between the stable modes again collapse; this alternating behavior repeats upon further increasing $\vec{U}^-(2\pi/a)$.

The band structures shown in Fig. 2 are only quantitatively altered (tilted) when a small uniform shear is imposed in addition to the periodic flow. However, for uniform shear ($s = 0.1, h = \infty, U_0^+ = 2.6, \text{Bo}^{-1} = 0.1$) flows with an existing KH instability (with unstable wave vectors near $k_x \sim \pi$) as determined by Eq. (11), the effect of an additional periodic flow in the lower fluid enhances these instabilities. However, when the uniform shear instabilities span $k_x \sim 2\pi$ ($s = 0.1, h = \infty, U_0^+ = 2.0, \text{Bo}^{-1} = 0.03$), where there is an open gap, the KH instability can be *suppressed* by a periodic flow $U^-(2\pi/a) = 0.20$, although more instabilities arise at higher k_x as well. These effects are shown using the extended zone scheme in Fig. 3. The structure of the dispersion relation is rather sensitive to the amount of underlying periodic flow and can change drastically with variation in any of the parameters.

The upward convex tongue of the KH instability in the $k_x - U_0^+$ plane is modified when $U^-(\vec{G} \neq 0)$ is added. For instabilities straddling the open gap Bragg

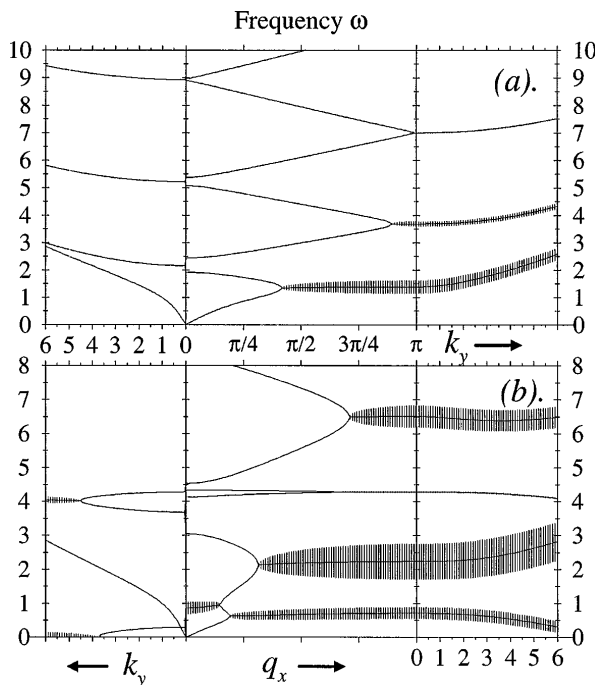


FIG. 2. Triptych depicting the band structure for periodic flow in the lower fluid ($s = 0, h = 2.0, \text{Bo}^{-1} = 0.01$). The central panel shows the dispersion relation in the q_x direction in the reduced zone scheme. (a) $U^-(2\pi/a) = 0.20$; (b) $U^-(2\pi/a) = 0.75$.

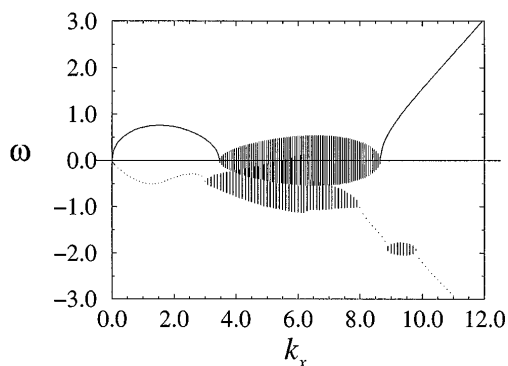


FIG. 3. Dispersion relation with and without an underlying periodic flow with a uniform ($\vec{U}_0^+ = 2.0$) overlying shear. Here, $h = \infty$, $\text{Bo}^{-1} = 0.03$, and $s = 0.1$. As a visual aid, we have imposed a Galilean shift $\Delta\vec{U}_0 = (\vec{U}_0^- + \vec{U}_0^+ s)/(1 + s)$ and plotted only one-half of each branch. The pure shear ($\vec{U}^- = 0$) dispersion relation is shown associated with the densely hatched instability region. The dotted line with sparsely hatched instability regions corresponds to the pure shear plus [$\vec{U}^-(\vec{G} \neq 0) = 0.2$].

planes, this tongue is shifted, with parts shifted upwards (resulting in destabilization) and downwards (resulting in stabilization). The discontinuity in growth rate is clearly shown in Fig. 3 near $k_x \approx 2\pi$. Moreover, other smaller tongues develop at higher q_x ($k_x \approx 3\pi$ in Fig. 3) corresponding to the closed gap instabilities that would occur in exclusively periodic flows (Fig. 2). The growth rates within the instability regions change as well as the delimiting instability regions. Qualitatively, these effects on KH instabilities result from suppression of the traveling unstable waves in KH shear flow, due to coupling to the standing waves of periodic flow, arising in the last term in **C** in Eq. (8). In other words, the interface experiences an effective shear depending upon the k_x considered.

For illustration we have chosen large $U^-(2\pi/a) = 0.2$ (≈ 9 cm/s for water). Smaller U^- gives qualitatively the same dispersion shown in Fig. 2(a). Fluids with low ν such as liquid He may better exhibit the predicted band structures since they would only be weakly dissipated. Experimentally, surface instabilities in the viscous, Marangoni driven limit have been observed optically [17]. Similarly, nonoscillatory deformations may be detected by studying specularly deflected laser light. Dynamic light scattering can also be used to detect the oscillatory modes. For example, heterodyne laser light scattering has been used to measure the spatial variation of propagating capillary waves [14]. The polar and azimuthal angles of incident light can be tuned so that various wave vectors of the dispersion relation presented can be readily probed.

The analogies between wave propagation in periodic media and surface wave propagation in periodic shear

flow configurations can be extended to consider more complicated periodic flow structures such as rectangular and hexagonal patterns. This may lead to insights with wide applicability, from Rayleigh-Bénard convection, Langmuir circulation, solar convection cells, and MHD surface Alfvén waves in the presence of periodic magnetic fields (in addition to flows) [7]. Furthermore, the influence of defects and disorder in the periodic surface flows [18] can be considered to study surface wave localization in the presence of random $\vec{U}(\vec{r}, 0)$ (and hence random **B**, **C**). For example, methods used to determine the complex spectrum density of states of random matrix operators [19] should yield information regarding the sea surface wave spectra in the presence of random underlying turbulent surface flows.

-
- [1] B. Whitham, *Linear and Nonlinear Waves* (Academic Press, New York, 1973).
 - [2] A. D. D. Craik, *Wave Interactions and Fluid Flows* (Cambridge University Press, Cambridge, 1985).
 - [3] L. G. Leal, *Laminar Flow and Convective Transport Processes* (Butterworth-Heinemann, Boston, 1992).
 - [4] D. D. Joseph and Y. Y. Renardy, *Fundamentals of Two-Fluid Dynamics. Part I: Mathematical Theory and Applications* (Springer-Verlag, New York, 1993).
 - [5] S. Leibovich, *Annu. Rev. Fluid Mech.* **15**, 391–427 (1983); C. J. R. Garrett, *J. Mar. Res.* **34**, 117–130 (1976).
 - [6] A. J. Szeri, *Mon. Weather Rev.* **124**, 341–342 (1996).
 - [7] J. A. Shercliff, *J. Fluid Mech.* **38**, 353–364 (1969).
 - [8] R. D. Benguria and M. C. Depassier, *Phys. Fluids* **30**, 1678–1682 (1987).
 - [9] L. C. Morland and P. G. Saffman, *J. Fluid Mech.* **252**, 383 (1993).
 - [10] J. P. McHugh, *Wave Motion* **16**, 23 (1992).
 - [11] N. W. Ashcroft and N. D. Mermin, *Solid State Physics* (W. B. Saunders, Philadelphia, 1976); J. D. Joannopoulos, R. D. Meade, and J. Winn, *Photonic Crystals: Molding the Flow of Light* (Princeton University Press, Princeton, New Jersey, 1995).
 - [12] T. Chou (to be published).
 - [13] A. Ajdari, *Phys. Rev. E* **53**, 4996–5005 (1996).
 - [14] T. Chou and D. R. Nelson, *J. Chem. Phys.* **101**, 9022–9032 (1994); K. Y. Lee, T. Chou, D. S. Chung, and E. Mazur, *J. Phys. Chem.* **97**, 12 876 (1993).
 - [15] W. H. Press, S. A. Teukolsky, W. T. Vetterling, and B. P. Flannery, *Numerical Recipes* (Cambridge University Press, Cambridge, England, 1992).
 - [16] J. C. Scott, *J. Fluid. Mech.* **116**, 283–296 (1982).
 - [17] S. J. van Hook *et al.*, *Phys. Rev. Lett.* **75**, 1938 (1995).
 - [18] J. M. Massaguer, *Phys. Fluids* **6**, 2304–2316 (1994); E. D. Siggia and A. Zippelius, *Phys. Rev. A* **24**, 1036–1049 (1981).
 - [19] J. T. Chalker and Z. J. Wang, *cond-mat/9704198*.